J. Shanghai Jiaotong Univ. (Sci.), 2014, 19(6): 736-746
DOI: 10.1007/s12204-014-1557-8

Numerical Study of Quasi-Static Crack Growth Problems Based on Extended Finite Element Method

ZHENG An-xing (郑安兴), *LUO Xian-qi** (罗先启)
(School of Naval Architecture, Ocean and Civil Engineering, Shanghai Jiaotong University, Shanghai 200240, China)

Abstract: The extended finite element method (XFEM) is a numerical method for modeling discontinuities within a classical finite element framework. Based on the algorithm of XFEM, the major factors such as integral domain factor and mesh density which all influence the calculation accuracy of stress intensity factor (SIF) are discussed, and the proper parameters to calculate the SIF are given. The results from the case analysis demonstrate that the crack path is the most sensitive to the crack growth increment size, and the crack path is not mesh-sensitive. A reanalysis method for the XFEM has been introduced. The example presented shows that there is a significantly reduced computational cost for each iteration of crack growth achieved by using the reanalysis method and the reanalysis approach has increasing benefits as the mesh density increases or the value of crack growth increments size decreases.

Key words: extended finite element method (XFEM), stress intensity factor (SIF), crack, level set, numerical methods
CLC number: TV 313 **Document code:** A

0 Introduction

A great amount of engineering practice shows that the structural instability is closely related to its internal crack propagation. Since the existence and propagation of the crack, the bearing capacity of the project structure is weakened to some extent and affects the safety of engineering structures. The crack problem has become one of the major factors affecting the quality and stability of engineering structures, and attracts more and more attention in engineering field and academic community. So studying the stability of crack and predicting the crack propagation path are of great significance in theory and practice for estimating the safety and reliability of engineering structures. Current numerical methods mainly include numerical manifold method[1], finite element method[2], meshless method[3] and boundary element method[4] for analyzing the crack propagation process and they show different characteristics in solving the mobile discontinuous problem of the crack propagation process. Numerical manifold method and finite element method need to set fine element at the crack tip, so, may lead to complex preprocessing and bad accuracy. Element-free method is without pre-processing such as mesh dissection, but the calculations of its shape functions and derivative cost greatly. The boundary element method must know the fundamental solution of control equation for the problem, but now the fundamental solution of the nonlinear problem is not easy to establish.

The extended finite element method (XFEM)[5] is a numerical method for modeling discontinuities within a standard finite element framework. It was first introduced by Professor Belytschko at Northwest University in 1999. Based on the partition of unity methods, mature theories and techniques of finite element method are inherited by XFEM. In the XFEM, a Heaviside function and the two-dimensional asymptotic crack-tip displacement fields are added to the finite element approximation to account for discontinuity of the crack surface and stress singularity near the crack tip respectively. This enables the domain to be modeled by finite elements without explicitly meshing the crack surfaces, and hence crack growth simulations can be carried out without remeshing. Since the unique advantage of XFEM for fracture analysis, it has developed applications rapidly and widely in the past a few years. Moës et al.[6] introduced a much more elegant technique by adapting an enrichment that includes the asymptotic near-tip field and a Heaviside function. Réthoré et al.[7] proposed a hybrid analytical and XFEM to study the propagation of curved mixed-mode cracks. Gordeliy and Anthony[8] used the XFEM to solve the elastic

Received date: 2013-07-09
Foundation item: the National Basic Research Program (973) of China (No. 2011CB013505) and the National Natural Science Foundation of China (No. 51279100)
***E-mail:** luoxianqi@sjtu.edu.cn

crack component of the elasto-hydrodynamic equations that govern the propagation of hydraulic fractures in an elastic medium. Zhu[9] presented a mathematical derivation of the enrichment functions in the XFEM for numerical modeling of strong and weak discontinuities. Liu et al.[10] developed a high-order XFEM based on the spectral element method for the simulation of dynamic fracture.

In this study, we apply the XFEM to crack problems in isotropic homogeneous media. Numerical examples are presented to demonstrate the accuracy of the numerical technique and to show its versatility of solving the challenging problems in computational fracture mechanics.

1 Extended Finite Element Method

1.1 XFEM Discrete Displacement Field

1.1.1 *XFEM Approximation for Cracks*

For modeling cracks in XFEM, the approximation function takes the following form:

$$\boldsymbol{u} = \sum_{i\in\Omega} N_i(\boldsymbol{p}) \left[\boldsymbol{u}_i + \underbrace{H(\boldsymbol{p})\boldsymbol{a}_i}_{i\in\Omega_\Gamma} + \underbrace{\sum_{l=1}^{4} F_l(\boldsymbol{p})\boldsymbol{b}_i^{(l)}}_{i\in\Omega_\Lambda} \right], \quad (1)$$

where, Ω is the entire domain; $N_i(\boldsymbol{p})$ is the traditional finite element shape function associated with node i; $\boldsymbol{p}$ is a sample (Gauss) point; $\boldsymbol{u}_i$ is the traditional degree of freedom; Ω_Γ is the domain cut by the crack; $H(\boldsymbol{p})$ is the Heaviside enrichment; $\boldsymbol{a}_i$ denotes the nodal enriched degree of freedom associated with the discontinuous Heaviside function; Ω_Λ is the domain containing the crack tip; $F_l(\boldsymbol{p})$ is the crack tip enrichment; $\boldsymbol{b}_i^{(l)}$ is nodal degree of freedom corresponding to the near-tip function.

For an element completely cut by a crack, the Heaviside enrichment function is used such that[6]

$$H(\boldsymbol{p}) = \begin{cases} +1, & (\boldsymbol{p}-\boldsymbol{p}^*)\cdot\boldsymbol{n} > 0 \\ -1, & \text{otherwise} \end{cases}, \quad (2)$$

where, $\boldsymbol{p}^*$ (lies on the crack) is the closest point to $\boldsymbol{p}$; $\boldsymbol{n}$ is the unit outward normal to the crack at $\boldsymbol{p}^*$.

The crack-tip enrichment function[11] in isotropic elasticity is

$$F_l(\boldsymbol{p}) = \sqrt{r}\Big[\sin\Big(\frac{\theta}{2}\Big) \quad \cos\Big(\frac{\theta}{2}\Big) \quad \sin(\theta)\cos\Big(\frac{\theta}{2}\Big) \quad \sin(\theta)\sin\Big(\frac{\theta}{2}\Big)\Big],$$

where (r,θ) are the polar coordinates in the local crack-tip coordinate system (see Fig. 1). Nodes in set Ω_Γ are the elements that their supports are split by the crack and nodes in set Ω_Λ belong to the elements that contain a crack tip. These nodes are enriched with the Heaviside and near-tip fields, respectively. When a node would be enriched by both $H(\boldsymbol{p})$ and $\boldsymbol{F}_l(\boldsymbol{p})$, only $\boldsymbol{F}_l(\boldsymbol{p})$ is used (see Fig. 2), in which the nodes with circle are enriched by the Heaviside step function, and the nodes with square are enriched by the crack tip enrichment functions.

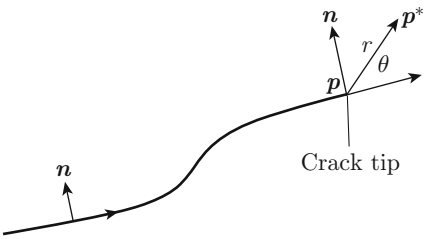

Fig. 1 The local coordinate system

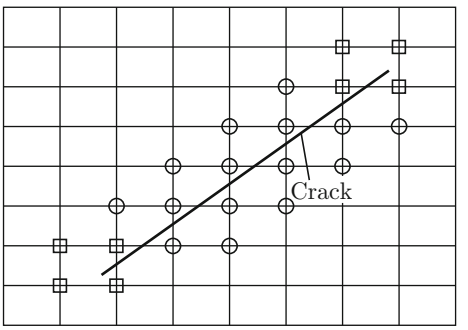

Fig. 2 The nodes enriched with the enrichment functions

1.1.2 *XFEM Approximation for Holes*

The enriched approximation for modeling holes in XFEM takes the following form:

$$\boldsymbol{u} = \sum_{i\in\Omega} N_i(\boldsymbol{p})\Big[\boldsymbol{u}_i + \underbrace{H(\boldsymbol{p})\boldsymbol{a}_i}_{i\in\Omega_\Gamma}\Big]. \quad (3)$$

The Heaviside jump function, $H(\boldsymbol{p})$, takes a value of 0 inside the hole and 1 outside the hole.

1.2 Discretized Equations

The discrete system of linear equations using the XFEM procedure in global form can be written by

$$\boldsymbol{K}\boldsymbol{d} = \boldsymbol{f}, \quad (4)$$

where $\boldsymbol{d}$ is the vector of nodal degrees of freedom for both classical and enriched ones, as defined in

$$\boldsymbol{d} = \big[\boldsymbol{u}_i \quad \boldsymbol{a}_i \quad \boldsymbol{b}_i^{(1)} \quad \boldsymbol{b}_i^{(2)} \quad \boldsymbol{b}_i^{(3)} \quad \boldsymbol{b}_i^{(4)}\big]^{\mathrm{T}}, \quad (5)$$

$\boldsymbol{K}$ and $\boldsymbol{f}$ are the global stiffness matrix and external force vector, respectively. The global stiffness matrix $\boldsymbol{K}$ can be considered as

$$\boldsymbol{K} = \begin{bmatrix} \boldsymbol{K}_{uu} & \boldsymbol{K}_{ua} & \boldsymbol{K}_{ub} \\ \boldsymbol{K}_{au} & \boldsymbol{K}_{aa} & \boldsymbol{K}_{ab} \\ \boldsymbol{K}_{bu} & \boldsymbol{K}_{ba} & \boldsymbol{K}_{bb} \end{bmatrix}. \quad (6)$$

The elemental stiffness matrix $\boldsymbol{K}_{\mathrm{e}}$ for any member of $\boldsymbol{K}$ may be calculated as

$$\boldsymbol{K}_{\mathrm{e}} = \int_{\Omega_{\mathrm{e}}} \boldsymbol{B}_k^{\mathrm{T}} \boldsymbol{D} \boldsymbol{B}_s \mathrm{d}\Omega, \tag{7}$$

where, $k, s = u, a, b$; Ω_{e} is an element such that the crack lies along the edges of these elements; $\boldsymbol{D}$ is the constitutive matrix for an isotropic linear elastic material; $\boldsymbol{B}_u$, $\boldsymbol{B}_a$ and $\boldsymbol{B}_b$ are the matrices of shape function derivatives,

$$\boldsymbol{B}_u = \begin{bmatrix} N_{i,x} & 0 \\ 0 & N_{i,y} \\ N_{i,y} & N_{i,x} \end{bmatrix},$$

$$\boldsymbol{B}_a = \begin{bmatrix} (N_i H)_x & 0 \\ 0 & (N_i H)_y \\ (N_i H)_y & (N_i H)_x \end{bmatrix},$$

$$\boldsymbol{B}_b = [\boldsymbol{B}_{b1} \quad \boldsymbol{B}_{b2} \quad \boldsymbol{B}_{b3} \quad \boldsymbol{B}_{b4}],$$

$$\boldsymbol{B}_{bl} = \begin{bmatrix} (N_i F_l)_x & 0 \\ 0 & (N_i F_l)_y \\ (N_i F_l)_y & (N_i F_l)_x \end{bmatrix},$$

$$l = 1, 2, 3, 4,$$

$N_{i,x}$ and $N_{i,y}$ are the derivatives of N_i with respect to x and y, respectively, $(N_i H)_x$ and $(N_i H)_y$ are the derivatives of $(N_i H)$ with respect to x and y, respectively, N_i is finite element shape function.

Force vector $\boldsymbol{f}$ is the equivalent node force for body force $\boldsymbol{b}$ and traction $\boldsymbol{t}$, as defined in

$$\boldsymbol{f} = [\boldsymbol{f}_u \quad \boldsymbol{f}_a \quad \boldsymbol{f}_{b1} \quad \boldsymbol{f}_{b2} \quad \boldsymbol{f}_{b3} \quad \boldsymbol{f}_{b4}]^{\mathrm{T}}, \tag{8}$$

and the vectors that appear in Eq. (8) are defined as

$$\left.\begin{aligned} \boldsymbol{f}_u &= \int_{\Gamma_{\mathrm{t}}} N_i \boldsymbol{t} \mathrm{d}\Gamma + \int_{\Omega_{\mathrm{e}}} N_i \boldsymbol{b} \mathrm{d}\Omega \\ \boldsymbol{f}_a &= \int_{\Gamma_{\mathrm{t}}} N_i H \boldsymbol{t} \mathrm{d}\Gamma + \int_{\Omega_{\mathrm{e}}} N_i H \boldsymbol{b} \mathrm{d}\Omega \\ \boldsymbol{f}_{bl} &= \int_{\Gamma_{\mathrm{t}}} N_i F_l \boldsymbol{t} \mathrm{d}\Gamma + \int_{\Omega_{\mathrm{e}}} N_i F_l \boldsymbol{b} \mathrm{d}\Omega \end{aligned}\right\}, \tag{9}$$

$$l = 1, 2, 3, 4,$$

where Γ_{t} is traction boundary.

1.3 Integration of Element with Discontinuity

The XFEM allows the mesh to be independent of the geometry. Hence, special care has to be taken while numerically integrating over the elements intersected by the discontinuity. A standard quadrature rule is not suitable for discontinuous functions, and it is the reason why the elements intersected by the crack are split into integration subdomains with their boundaries aligned with the crack, as illustrated in Ref. [6], in such a way that there is no discontinuity in any of the subdomains. Integration would then be performed over each subdomain, and a series of integrations over continuous domains would be achieved. The common number of Gauss points for integration in each triangular subdomain with the Heaviside enrichment is 3 while that for the crack tip enrichment functions is 7. An example of an element completely cut by a crack as well as containing a crack tip and the associated subdomains for integration is shown in Fig. 3.

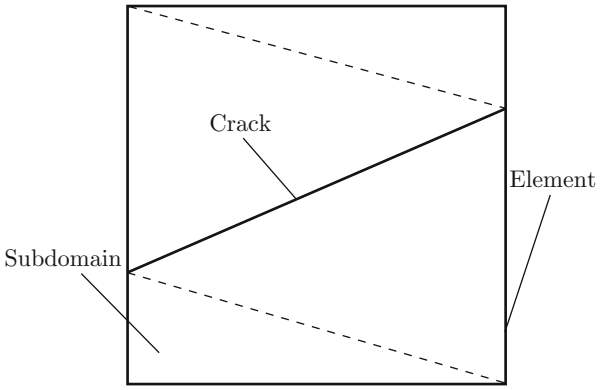

(a) Element cut by crack divided into four continuous subdomains

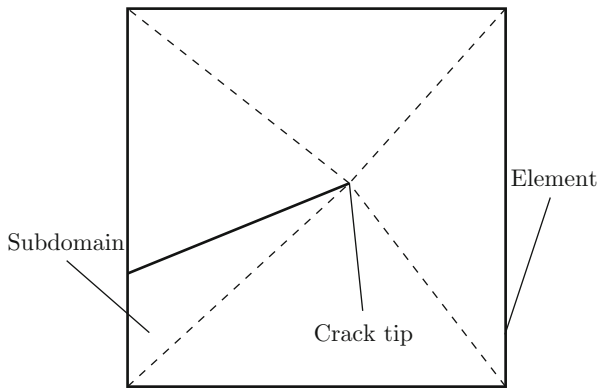

(b) Element containing crack tip divided into five continuous subdomains

Fig. 3 Elements containing a discontinuity and the continuous subdomains for integration

1.4 The Level Set Method

1.4.1 *Level Sets for Cracks*

The level set method introduced by Osher and Sethian[12] as a numerical method can be used to track the evolution of interfaces and shapes. XFEM and level set method work together naturally for crack growth modeling. Since the crack is an open curve, two orthogonal level set functions are required to represent it. The first level set function $\varphi(\boldsymbol{p}, t)$ is normal to the crack and the zero level set of this function represents the crack surface. The other level set function $\phi(\boldsymbol{p}, t)$ is tangent to the crack at its tip and represents the crack

location at any time t.

The level set function $\varphi(\boldsymbol{p},t)$ which represents the crack surface can be written as

$$\varphi(\boldsymbol{p},t)=\pm\min\|\boldsymbol{p}-\boldsymbol{p}_i\|, \tag{10}$$

where $\varphi(\boldsymbol{p},t)$ is the signed-distance to the interface and $\boldsymbol{p}_i$ is the location of the ith crack tip. The sign of the minimum distance depends on which side of the interface where a point $\boldsymbol{p}$ is located.

The level set function $\phi(\boldsymbol{p},t)$ that represents the crack tip is initially defined by

$$\phi_i(\boldsymbol{p},0)=(\boldsymbol{p}-\boldsymbol{p}_i)\cdot\boldsymbol{t}', \tag{11}$$

where $\boldsymbol{t}'$ is a unit vector tangent to the crack at its tip, and $\boldsymbol{p}_i$ is also the location of the ith crack tip. The initial level set functions φ and ϕ_i, and the representation of the crack are shown in Fig. 4.

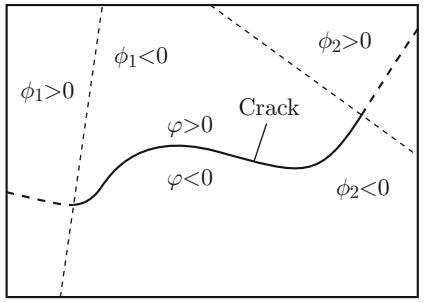

Fig. 4 Crack described by the level set method

For the case of more than one crack tip, it is convenient to define a single function $\phi(\boldsymbol{p},t)$ for the crack tip level set representation by

$$\phi(\boldsymbol{p},t)=\max\phi_i(\boldsymbol{p},t). \tag{12}$$

The function ϕ allows us to define the location of the crack using only one function whether a crack has one or two tips. In other words, a crack is defined as the set

$$\{\boldsymbol{p}:\varphi(\boldsymbol{p},t)=0 \text{ and } \phi(\boldsymbol{p},t)\leqslant 0\}. \tag{13}$$

1.4.2 *Level Sets Update for Cracks*

Crack growth is modelled by appropriately updating the ϕ_i and φ functions, then reconstructing the updated ϕ function[13]. The evolution of ϕ_i and φ is determined by the crack growth direction θ_c. In each step, the crack tip displacement vector is given as $\boldsymbol{F}=(F_x,F_y)$ and the current crack tip is given by the coordinates (x_i,y_i). The following steps describe the simple procedure of evolution of the level set functions $\phi_i^{(n)}$ and $\varphi^{(n)}$ at the step n:

(1) $\boldsymbol{F}$ is not necessarily orthogonal to the zero level set of $\phi_i^{(n)}$. For this reason, we must first rotate $\phi_i^{(n)}$ so that $\boldsymbol{F}$ is orthogonal. Here, $\phi_i^{(n)}$ after rotation is referred to as $\hat{\phi}_i$ and given by

$$\hat{\phi}_i=\frac{(x-x_i)F_x}{\|\boldsymbol{F}\|}+\frac{(y-y_i)F_y}{\|\boldsymbol{F}\|}. \tag{14}$$

(2) The crack is extended by computing new values of $\varphi^{(n+1)}$:

$$\varphi^{(n+1)}=\begin{cases}\varphi^{(n)}, & \hat{\phi}_i<0\\ \pm\left|\dfrac{(x-x_i)F_y}{\|\boldsymbol{F}\|}-\dfrac{(y-y_i)F_x}{\|\boldsymbol{F}\|}\right|, & \hat{\phi}_i\geqslant 0\end{cases}. \tag{15}$$

(3) The updated location of the crack tip can be computed by

$$\phi_i^{(n+1)}=\hat{\phi}_i-\Delta t\|\boldsymbol{F}\|, \tag{16}$$

where Δt is the elapsed time between $\phi_i^{(n)}$ and $\phi_i^{(n+1)}$.

(4) Once all $\phi_i^{(n+1)}$ corresponding to a crack are updated, $\phi_i^{(n+1)}$ is updated using Eq. (12).

The location of the new crack tip i can now be determined by finding the intersection of the zero level sets of $\phi_i^{(n+1)}$ and $\varphi^{(n+1)}$. The sketch map of level set function update is illustrated in Fig. 5.

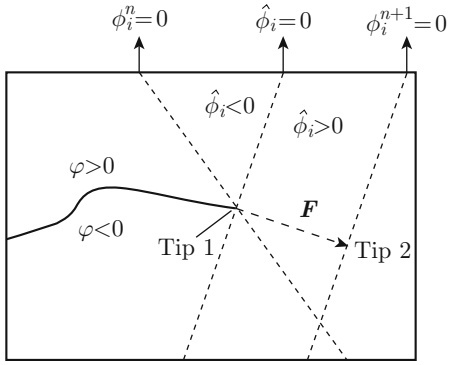

Fig. 5 Level set function update

1.4.3 *Level Sets for Circular Holes*

For our purposes, the interface is static, so we only use the level set theory for representing circular holes which can be written as

$$\varphi(\boldsymbol{p},0)=\min_{\boldsymbol{p}_c^{(i)}\in\Omega_c^{(i)}}\left\{\|\boldsymbol{p}-\boldsymbol{p}_c^{(i)}\|-r_c^{(i)}\right\},\quad i=1,2,\cdots,n_c, \tag{17}$$

where $\Omega_c^{(i)}$ is the domain of the ith hole; n_c is the number of circular holes; $\boldsymbol{p}_c^{(i)}$ and $r_c^{(i)}$ are the center location and radius of the ith hole. The level set function is positive or negative as illustrated in Fig. 6.

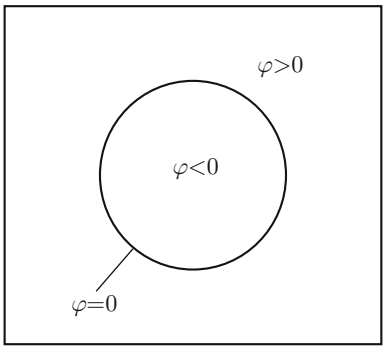

Fig. 6 Hole described by the level set method

1.4.4 *Definition and Selection of the Enriched Nodes*

Level sets contain all the necessary information for modeling crack, and allow crack grow over a fixed mesh. Further, they facilitate selection of nodes for enrichment. The selection of enriched nodes can be simplified by the use of the level set functions ϕ and φ. Let, $\phi_{\max}$ and $\phi_{\min}$ (correspondingly $\varphi_{\max}$ and $\varphi_{\min}$) be the maximum and minimum values of ϕ (correspondingly φ) at the nodes of a given element. Then an element is enriched with the Heaviside enrichment when $\phi_{\max} < 0$ and $\varphi_{\max}\varphi_{\min} \leqslant 0$, and with the crack tip enrichment when $\phi_{\max}\phi_{\min} \leqslant 0$ and $\varphi_{\max}\varphi_{\min} \leqslant 0$.

2 Crack Growth and Stress Intensity Factor Evaluation

2.1 Crack Growth

There are several criteria for predicting crack growth direction in homogeneous materials. The maximum circumferential stress criterion[6] which is a commonly used criterion is adopted herein. According to this criterion, the crack growth occurs in a direction perpendicular to the maximum principal stress. Thus, at each crack tip, the angle of crack growth θ_{c} is given by

$$\theta_{\mathrm{c}} = 2\arctan\frac{1}{4}\left(\frac{K_{\mathrm{I}}}{K_{\mathrm{II}}} \pm \sqrt{\left(\frac{K_{\mathrm{I}}}{K_{\mathrm{II}}}\right)^2 + 8}\right), \tag{18}$$

where K_{I} and K_{II} are the mixed-mode stress intensity factors (SIFs).

According to this criterion, the equivalent mode-I SIF is obtained as

$$K_{\mathrm{I}}^{\mathrm{eq}} = \frac{1}{2}\cos\left(\frac{\theta_{\mathrm{c}}}{2}\right)[K_{\mathrm{I}}(1+\cos\theta_{\mathrm{c}}) - 3K_{\mathrm{II}}\sin\theta_{\mathrm{c}}]. \tag{19}$$

2.2 Evaluation of SIFs

2.2.1 *Obtaining SIFs from Interaction Integral*

An interaction integral approach is used to evaluate the SIF at the tip of the crack. The coordinates are taken to be the local crack tip coordinates with the x_1-axis parallel to the crack faces. The modified interaction integral for XFEM can be written in the domain form as[14]

$$I^{(1,2)} = \int_A \left[\sigma_{ij}^{(1)}\frac{\partial u_i^{(2)}}{\partial x_1} + \sigma_{ij}^{(2)}\frac{\partial u_i^{(1)}}{\partial x_1} - W^{(1,2)}\delta_{1j}\right]\frac{\partial q}{\partial x_j}\mathrm{d}A, \tag{20}$$

where, $I^{(1,2)}$ is called the interaction integral for states 1 and 2; σ_{ij} represents stress component; u_i denotes displacement component; δ_{1j} is the Kronecker delta; A is an area surrounding the crack tip and q is a weighting function; $W^{(1,2)}$ represents the strain energy density for states 1 and 2. The states 1 and 2 depict the actual state and the auxiliary state, respectively. Field variables for the actual state are obtained by the XFEM solution and those for auxiliary state are chosen as the crack tip asymptotic fields[11]. Strain energy density $W^{(1,2)}$ is given as

$$W^{(1,2)} = \frac{1}{2}(\sigma_{ij}^{(1)}\varepsilon_{ij}^{(2)} + \sigma_{ij}^{(2)}\varepsilon_{ij}^{(1)}), \tag{21}$$

where ε_{ij} represents strain component.

Expanding and rearranging terms from Eq. (20) gives

$$\begin{aligned} I^{(1,\mathrm{aux})} = \int_A \Big[\Big(&\sigma_x\frac{\partial u_x^{\mathrm{aux}}}{\partial x} + \tau_{xy}\frac{\partial u_y^{\mathrm{aux}}}{\partial x} + \sigma_x^{\mathrm{aux}}\frac{\partial u_x}{\partial x} + \\ &\tau_{xy}^{\mathrm{aux}}\frac{\partial u_y}{\partial x} - \sigma_{ij}\varepsilon_{ij}^{\mathrm{aux}}\Big)\frac{\partial q}{\partial x} + \Big(\tau_{xy}\frac{\partial u_x^{\mathrm{aux}}}{\partial x} + \\ &\sigma_y\frac{\partial u_y^{\mathrm{aux}}}{\partial x} + \tau_{xy}^{\mathrm{aux}}\frac{\partial u_x}{\partial x} + \sigma_y^{\mathrm{aux}}\frac{\partial u_y}{\partial x}\Big)\frac{\partial q}{\partial y}\Big]\mathrm{d}A, \end{aligned} \tag{22}$$

where, superscript "aux" denotes auxiliary fields; σ_x and σ_y represent stress components on the x and y axes, respectively; τ_{xy} is the shear stress.

The interaction energy integral is related to the SIFs as follows[15]:

$$I^{(1,2)} = \frac{2}{E^*}(K_{\mathrm{I}}^{(1)}K_{\mathrm{I}}^{(2)} + K_{\mathrm{II}}^{(1)}K_{\mathrm{II}}^{(2)}), \tag{23}$$

where E^* is defined in terms of material parameters E (elastic modulus) and ν (Poisson's ratio) as

$$E^* = \begin{cases} E, & \text{plane stress} \\ \dfrac{E}{1-\nu^2}, & \text{plane strain} \end{cases}. \tag{24}$$

To obtain mode-I SIF for state 1, the auxiliary state (state 2) is chosen to be the pure mode-I condition. Substituting $K_{\mathrm{I}}^{(2)} = 1$ and $K_{\mathrm{II}}^{(2)} = 0$ into Eq. (23) gives

$$K_{\mathrm{I}}^{(1)} = \frac{E^*}{2}I^{(1,\text{mode-I})}, \tag{25}$$

where $I^{(1,\text{mode-I})}$ is the interaction integral for $K_{\mathrm{I}}^{(2)} = 1$ and $K_{\mathrm{II}}^{(2)} = 0$.

A similar procedure can also be followed such that $K_{\mathrm{II}}^{(1)}$ is given by

$$K_{\mathrm{II}}^{(1)} = \frac{E^*}{2} I^{(1,\text{mode-II})}, \tag{26}$$

where $I^{(1,\text{model-II})}$ is the interaction integral for $K_{\mathrm{I}}^{(2)} = 0$ and $K_{\mathrm{II}}^{(2)} = 1$. Once SIFs are obtained, fracture parameters θ_{c} can be easily computed.

2.2.2 *Integral Domain Selection*

For the numerical evaluation of the interaction integral, the domain A is set to be all elements which have a node within a ball of radius r about the crack tip (see Fig. 7). The integral domain A may be written as

$$R = R_k h_{\mathrm{local}}, \tag{27}$$

where, h_{local} is designated as the characteristic length of an element touched by the crack tip and it is calculated as the square root of the element area for two-dimensional analysis; R_k is the integral domain factor and it can regulate integral domain size. We study about the effect of integral domain factor on SIF.

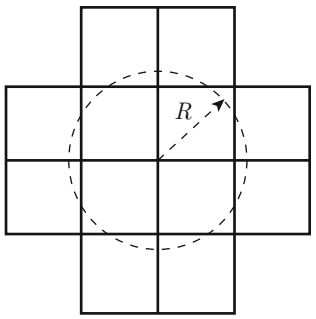

Fig. 7 Elements selected about the crack tip for calculation of the interaction integral

3 Reanalysis Method

Reanalysis method is intended to accurately evaluate the structural responses for successive modifications in design or optimization, without repeatedly solving the complete system of modified analysis equations so that the computational cost can be significantly reduced[15]. A reanalysis method for the XFEM is introduced here.

Recall that the approximation of the displacement for cracks in XFEM takes the form

$$\boldsymbol{u} = \sum_{i\in\Omega} N_i(\boldsymbol{p}) \left[\boldsymbol{u}_i + \underbrace{H(\boldsymbol{p})\boldsymbol{a}_i}_{i\in\Omega_\Gamma} + \underbrace{\sum_{l=1}^{4} F_l(\boldsymbol{p})\boldsymbol{b}_i^{(l)}}_{i\in\Omega_\Lambda} \right], \tag{28}$$

and the corresponding finite element stiffness matrix takes the form

$$\boldsymbol{K} = \begin{bmatrix} \boldsymbol{K}_{uu} & \boldsymbol{K}_{ua} & \boldsymbol{K}_{ub} \\ \boldsymbol{K}_{ua}^{\mathrm{T}} & \boldsymbol{K}_{aa} & \boldsymbol{K}_{ab} \\ \boldsymbol{K}_{ub}^{\mathrm{T}} & \boldsymbol{K}_{ab}^{\mathrm{T}} & \boldsymbol{K}_{bb} \end{bmatrix}. \tag{29}$$

It can be noticed from Eqs. (28) and (29) that the stiffness component associated with the traditional finite element approximation is not a function of the crack location, so it implies that the $\boldsymbol{K}_{uu}$ component of the stiffness matrix will be constant at each iteration of crack growth. This implies that the changing portion of the stiffness matrix is limited to the enriched portion, which will be small compared with the unenriched portion[16]. Furthermore, it can also be noticed that the Heaviside enrichment term $\boldsymbol{K}_{aa}$ is a function of the crack location within an element; once an element has been enriched with the Heaviside enrichment, its stiffness value will not change in any future iterations. The stiffness components containing subscript a will be constant for future iterations of crack growth. Figure 8 illustrates the portion of stiffness matrix that is kept constant from the previous iteration and the other portions that have to be modified due to crack growth. So we can use this property to maximize the recycling computational resources during crack growth simulation. For the first iteration of the quasi-static solution procedure, the full XFEM stiffness matrix is calculated. In subsequent iterations, only the changed portion of the XFEM stiffness matrix is calculated (i.e. the new Heaviside and crack tip enrichment components). This solution procedure significantly reduces the computational time required for the simulation of crack growth in the XFEM environment.

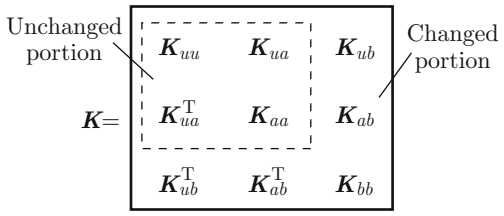

Fig. 8 Reanalysis of XFEM stiffness matrix due to crack growth

4 Numerical Examples

In this section, we present several numerical examples of cracks and crack growth under the assumptions of plane strain (two-dimensional) elasticity. The calculation of the stress intensity factors is performed with the domain form of the interaction integral as detailed in the previous section. The direction of crack growth is determined from the maximum circumferential stress criterion.

4.1 Center Crack in a Finite Plate

To illustrate the versatility and effectiveness of this method, SIFs are calculated for a finite plate with a center crack under uniaxial tension. The geometry and specifications for center crack numerical model are shown in Fig. 9. The material properties used in the analysis are chosen to be elastic modulus $E = 20\,\text{MPa}$ and Poisson's ratio $\nu = 0.3$. The full domain is a plate with height $h = 8\,\text{m}$, width $w = 4\,\text{m}$ and a center crack of length $2c = 1\,\text{m}$. The applied stress is $\sigma = 1\,\text{Pa}$. Square plane strain quadrilateral elements with a structured mesh are used.

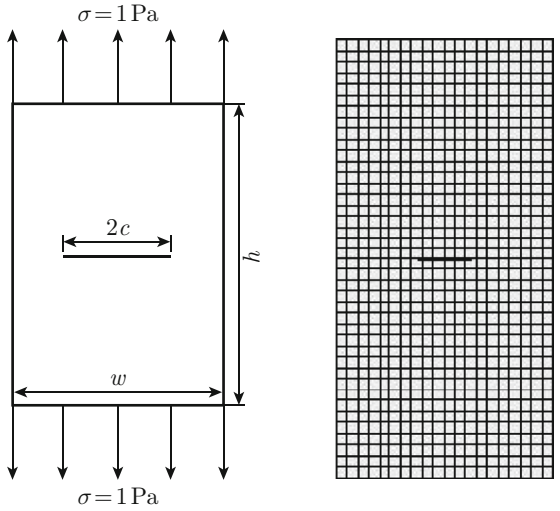

(a) Model geometry of center crack (b) Meshes for center crack

Fig. 9 Center crack numerical model

The theoretical SIF for a center crack in a finite plate under tension is

$$K_{\text{I}}^{\text{exac}} = \left[1 + 0.128\left(\frac{2c}{w}\right) - 0.288\left(\frac{2c}{w}\right)^2 + 1.525\left(\frac{2c}{w}\right)^3\right]\sigma\sqrt{\pi c}. \tag{30}$$

The theoretical mode-I SIF can be calculated by Eq. (30) of 1.300 4. The normalized SIF is defined as

$$K_{\text{I}}^{\text{n}} = \frac{K_{\text{I}}^{\text{XFEM}}}{K_{\text{I}}^{\text{exac}}}, \tag{31}$$

where $K_{\text{I}}^{\text{exac}}$ is given by Eq. (30), and $K_{\text{I}}^{\text{XFEM}}$ is the value calculated by the XFEM analysis using the domain form of the interaction integral. The normalized results for the various mesh densities and integral domain factors are given in Tables 1 and 2.

Figure 10 shows the effect of mesh density on SIF with the integral domain factor of 3. It can be noticed from Fig. 10 that the good accuracy of computational results can be obtained in the case of coarse mesh and the error decreases with the increase of element number. The mesh density has no more influence on the SIF when the element number around 5 000. The effect of integral domain factor on SIF is shown in Fig. 11

Table 1 Normalized SIF values for various mesh densities

Mesh density	K_{I}^{n}
128	0.936 6
800	0.962 1
2592	0.978 9
5 408	0.985 7
7 200	0.987 9
11 552	0.990 8

Table 2 Normalized SIF values for various integral domain factors

R_k	K_{I}^{n}
1.5	0.992 2
2.0	0.989 6
2.5	0.986 9
3.0	0.985 8
3.5	0.985 4
4.0	0.985 4
4.5	0.985 9
5.0	0.985 9

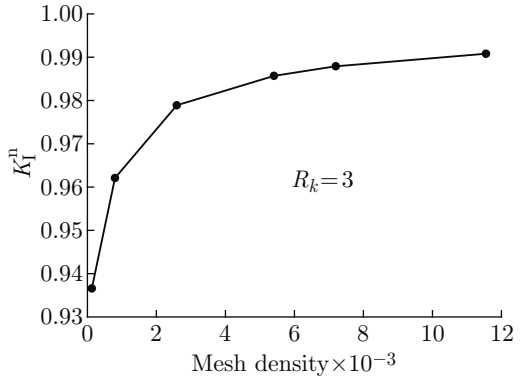

Fig. 10 The effect of mesh density on SIF

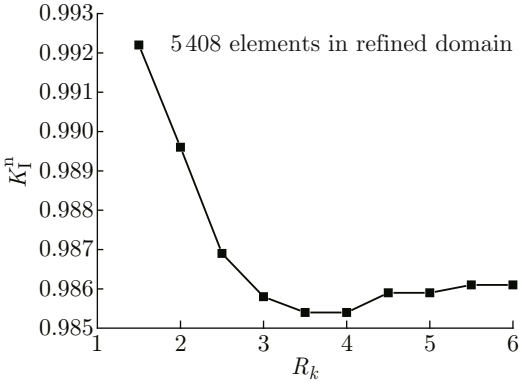

Fig. 11 The effect of integration factor on SIF

with a uniform mesh consisting of 5 408 elements in the numerical model. It can be noticed from Fig. 11 that the calculation result is not stable when the integral domain factor is less than 3 and the calculation result is stable when the integral domain factor is more than 3. Therefore, we suggest that the value of integral domain factor should be 3.

Figure 12 shows the SIFs for various crack lengths with the integral domain factor of 3 and elements of 5 408 in the full domain. It can be noticed from Fig. 12 that the SIF results obtained by XFEM agree well with the exact solution for the entire crack length of $2c/w$.

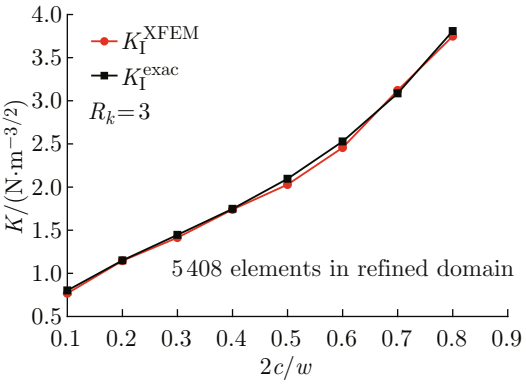

Fig. 12 The SIFs for various crack lengths

4.2 Edge Crack in a Finite Plate with a Hole

An example is provided here where an XFEM analysis is performed on a plate with a hole as shown in Fig. 13(a). The chosen plate dimensions are a width of 4 m and a height of 4 m with a hole of 0.5 m radius, and the distances between center and crack surface is taken as $d = 1$ m. The edge crack has an initial length of 1 m. The material properties for the plate are chosen as $E = 20$ GPa, $\nu = 0.3$ and the plane fracture toughness $K_\mathrm{Ic} = 280\,\mathrm{kN/m^{3/2}}$. The applied stress is $\sigma = 0.1$ MPa.

In the numerical model, a uniform mesh consisting of 60 element × 60 element is considered and quasi-static crack growth is governed by the maximum circumferential stress criterion. In the initial study, the change in crack length for each iteration is taken to be a constant crack growth increment $\Delta c = 0.2$ m, and the cracks are grown for twelve steps. Table 3 gives the position and SIFs of the top crack tip at each stage of the simulation. In Fig. 13(b), a representative crack growth simulation (60 mesh × 60 mesh) for 12 steps is shown. It can be seen from Fig. 13(b) that the crack grows close to the hole, and then deviates from it. The reason may be that the proximity of stress field created by the hole is able to deflect the crack path from a straight direction. Our results are similar to those in Ref. [17].

Figure 14 shows the relationship between the SIF at the crack tip and the crack growth length during the crack propagation. It can be seen from Fig. 14 that the mode-I SIF at the crack tip increases with the increase

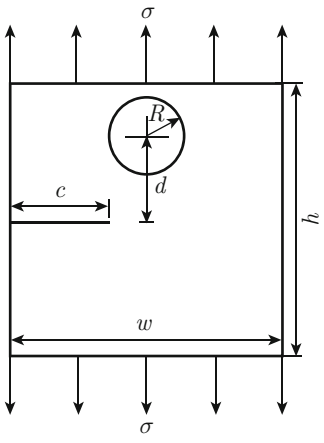

(a) Geometry

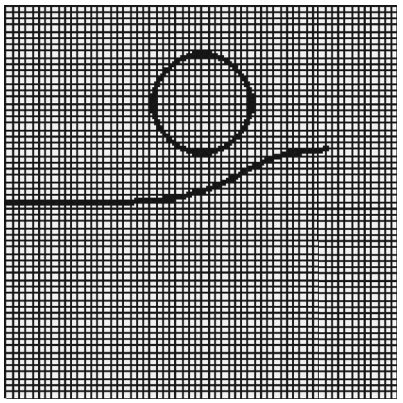

(b) Crack propagation path

Fig. 13 Numerical model

Table 3 Position and SIFs for crack tip

Step	x_i/m	y_i/m	K_I/ $(\mathrm{N\cdot m^{-3/2}})$	K_II/ $(\mathrm{N\cdot m^{-3/2}})$
Initial	1.000 0	2.000 0	$3.442\,1\times10^{5}$	$3.228\,5\times10^{3}$
1	1.200 0	1.996 2	$4.263\,2\times10^{5}$	$-1.139\,2\times10^{4}$
2	1.399 8	2.003 2	$5.202\,4\times10^{5}$	$-1.438\,5\times10^{4}$
3	1.599 0	2.021 1	$6.259\,9\times10^{5}$	$-2.269\,8\times10^{4}$
4	1.796 4	2.053 4	$7.439\,1\times10^{5}$	$-3.363\,7\times10^{4}$
5	1.990 1	2.103 3	$8.768\,1\times10^{5}$	$-4.492\,5\times10^{4}$
6	2.177 7	2.172 6	$1.015\,3\times10^{6}$	$-5.018\,3\times10^{4}$
7	2.357 6	2.260 0	$1.160\,8\times10^{6}$	$-2.976\,8\times10^{4}$
8	2.532 8	2.356 5	$1.331\,2\times10^{6}$	$4.013\,6\times10^{4}$
9	2.713 4	2.442 3	$1.621\,9\times10^{6}$	$1.383\,8\times10^{5}$
10	2.905 9	2.496 7	$2.166\,6\times10^{6}$	$1.609\,5\times10^{5}$
11	3.104 2	2.522 3	$3.069\,4\times10^{6}$	$1.067\,6\times10^{5}$
12	3.303 9	2.534 2	$4.702\,8\times10^{6}$	$8.117\,2\times10^{4}$

of crack growth length and the mode-II SIF is much smaller than the mode-I SIF. The results show that the crack propagation is non-steady propagation and mode-I crack propagation is the main form of crack propagation.

The purpose of this study is to attempt to assess the effect of the mesh density and crack growth increments Δc on the predicted crack path in a finite plate with a hole, as shown in Fig. 15. All the cracks are grown to 2.4 m from the initial crack tip in this example. Three different meshes and three different crack growth increment sizes are used. In Fig. 15(a), crack growth simulations for three different meshes are presented ($\Delta c = 0.2$ m); it is observed that under the given simulation conditions, the crack path is not mesh-sensitive. The influence of the crack growth increment Δc on the simulation is depicted in Fig. 15(b). The results clearly indicate that Δc has the most pronounced effect on crack growth.

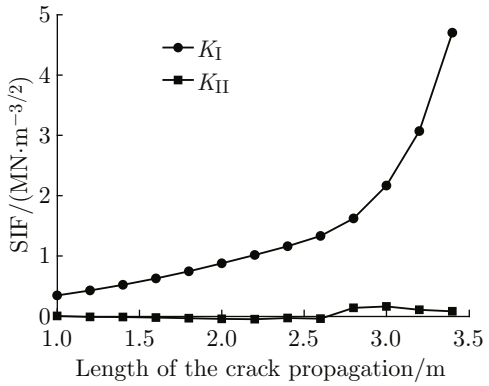

Fig. 14 Relationship between the SIF at the crack tip and the crack propagation length

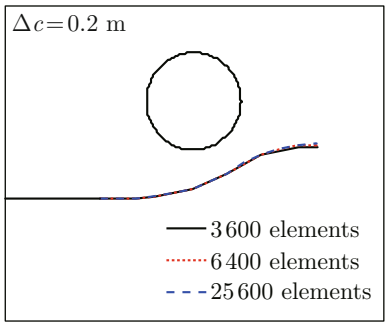

(a) Effect of mesh density

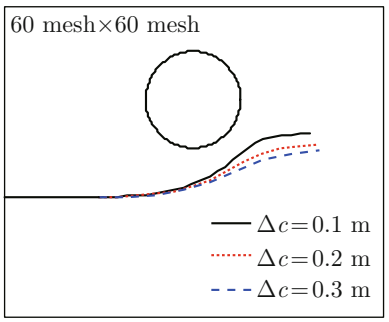

(b) Effect of crack growth increment Δc

Fig. 15 Parametric effect of simulated crack paths in a finite plate with a hole

4.3 Analysis of Reanalysis Method

By the above analysis, mesh density and crack growth increments Δc have an impact on accuracy of XFEM analysis results. If large value of Δc is selected, it may not accurately predict crack path. On the other hand, very small value of Δc and fine mesh will greatly increase computational burden. A reanalysis method for the XFEM is used here for modeling quasi-static growth. The reanalysis method allows for one to consider a smaller crack growth increment, which should lead to a better prediction of the crack growth path within a comparable computational budget. The first step in evaluating the proposed reanalysis method is to consider an edge crack in a finite plate with a hole that will allow us to assess the savings from the reanalysis method. An edge crack in a finite plate with a hole under uniaxial tension is shown in Fig. 13(a). All the parameters including geometry and material properties for the simulation are the same as the above example.

The test is to perform 12 iterations of crack growth with a constant crack growth increment $\Delta c = 0.2$ m and a uniform mesh consists of 160 element × 160 element in the numerical model. The total computational time for the case without reanalysis is 61 s, while the total time with reanalysis is 38 s. Figure 16 shows the comparison of computational time with and without reanalysis in each iteration. It is observed from Fig. 16 that the computational time for each iteration of crack growth is drastically decreased by using the reanalysis method.

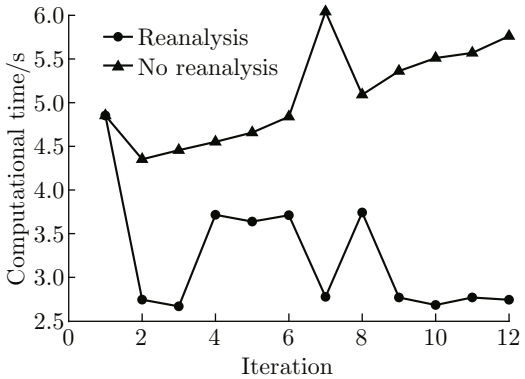

Fig. 16 Comparison of computational time with and without reanalysis

The second consideration is to study the effect of the mesh density and crack growth increments Δc on the reanalysis method. All the cracks are grown to

2.4 m from the initial crack tip in this example. Figure 17 shows the effect of the mesh density on the reanalysis method. There are several observations which one can make from Fig. 17. The computational time for initial iteration increases as the number of element increases. The reanalysis is a bit more expensive as the number of element increases, but still nearly linear and still much less expensive than the initial iteration. When the mesh density has an increased level of refinement, the largest savings can be achieved.

Figure 18 shows the effect of the crack growth increment size on the reanalysis method. Several observations can be obtained from Fig. 18. The computational time for initial iteration is unchanged as the value of crack growth increment size increases. The reanalysis is a bit more expensive as the value of crack growth increment size decreases, but still much less expensive than the initial iteration. When the value of crack growth increment size has a decreased level of refinement, the largest savings can be achieved.

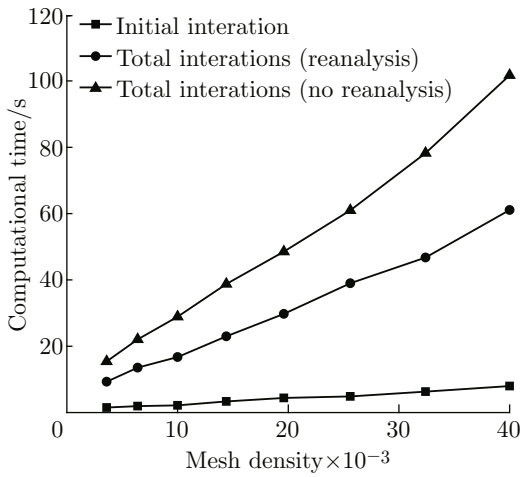

Fig. 17 Comparison of mesh density to cost of reanalysis for constant $\Delta c = 0.2$ m

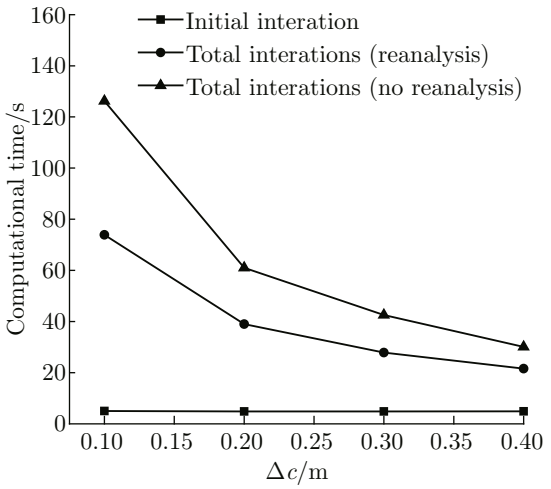

Fig. 18 Comparison of crack growth increment to cost of reanalysis for 160 × 160 elements

5 Conclusion

The XFEM allows for discontinuities to be represented independent of the finite element mesh by incorporating enrichment functions into the displacement approximation through the partition of unity finite element method. Thus crack growth problems can be solved with minimal remeshing, and crack modeling can be carried out without the need to mesh the crack surface. We have presented numerical applications of the XFEM to demonstrate the efficacy of our implementation and to show the capabilities of solving the challenging problems in computational fracture mechanics.

Our focus in this study is on computational fracture applications in isotropic homogeneous materials. Accurate stress intensity factors are calculated by the XFEM analysis using the domain form of the interaction integral for a finite plate with a center crack under uniaxial tension. In addition, a preliminary parameter study on the influence of the integral domain factor and mesh density used for stress intensity computation is performed. The study reveals that mesh density does not significantly affect the accuracy of SIFs when the element number reaches a certain quality (such as 5 000) and the integral domain factor has a great impact on the accuracy of SIFs. Therefore, we suggest that the value of integral domain factor should be 3.

The crack growth capabilities of the XFEM are demonstrated through growth simulations in a finite plate with a hole. The effects of mesh density and crack growth increment size are considered with respect to the convergence of the crack propagation path. The numerical results reveal that the crack path is the most sensitive to the crack growth increment size and the crack path is not mesh-sensitive.

A reanalysis method for the XFEM has been introduced. There is a significantly reduced computational cost for each iteration of crack growth achieved by using the reanalysis method. The effect of mesh density and crack growth increment size on the reanalysis method is studied and it is found that the largest savings are achieved when the mesh has an increased level of refinement or the value of crack growth increment size has a decreased level of refinement.

References

[1] Wu Z J, Wong L N Y. Frictional crack initiation and propagation analysis using the numerical manifold method [J]. *Computers and Geotechnics*, 2012, **39**: 38-53.

[2] Branco R, Antunes F V. Finite element modelling and analysis of crack shape evolution in mode-I fatigue middle cracked tension specimens [J]. *Engineering Fracture Mechanics*, 2008, **75**(10): 3020-3037.

[3] Wu S, Fang S. Modeling cohesive cracks with meshless method [J]. *International Journal of Damage Mechanics*, 2009, **18**(8): 721-737.

[4] Wen P H, Aliabadi M H. Dual boundary element method for modelling curved crack paths [J]. *International Journal of Fracture*, 2012, **176**(1): 127-133.

[5] Belytschko T, Black T. Elastic crack growth in finite elements with minimal remeshing [J]. *International Journal for Numerical Methods in Engineering*, 1999, **45**: 601-620.

[6] Moës N, Dolbow J, Belytschko T. A finite element method for crack growth without remeshing [J]. *International Journal for Numerical Methods in Engineering*, 1999, **46**(1): 131-150.

[7] Réthoré J, Roux S, Hild F. Mixed-mode crack propagation using a hybrid analytical and extended finite element method [J]. *Comptes Rendus Mecanique*, 2010, **338**: 121-126.

[8] Gordeliy E, Peirce A. Coupling schemes for modeling hydraulic fracture propagation using the XFEM [J]. *Computer Methods in Applied Mechanics and Engineering*, 2013, **253**: 305-322.

[9] Zhu Q Z. On enrichment functions in the extended finite element method [J]. *International Journal for Numerical Methods in Engineering*, 2012, **91**: 186-217.

[10] Liu Z L, Menouillard T, Belytschko T. An XFEM/spectral element method for dynamic crack propagation [J]. *International Journal of Fracture*, 2011, **169**(2): 183-198.

[11] Fleming M, Chu Y A, Moran B, et al. Enriched element-free Galerkin methods for crack tip fields [J]. *International Journal for Numerical Methods in Engineering*, 1997, **40**(8): 1483-1504.

[12] Osher S, Sethian J A. Fronts propagating with curvature dependent speed: Algorithms based on Hamilton-Jacobi formulations [J]. *Journal of Computational Physics*, 1988, **79**(1): 12-49.

[13] Stolarska M, Chopp D L, Moës N, et al. Modelling crack growth by level sets in the extended finite element method [J]. *International Journal for Numerical Methods in Engineering*, 2001, **51**: 943-960.

[14] Sukumar N, Prèvost J H. Modeling quasi-static crack growth with the extended finite element method. Part I. Computer implementation [J]. *International Journal of Solids and Structures*, 2003, **40**(26): 7513-7537.

[15] Wu B, Li Z. Static reanalysis of structures with added degrees of freedom [J]. *Communications in Numerical Methods in Engineering*, 2006, **22**: 269-281.

[16] Pais M J, Yeralan S N, Davis T A, et al. An exact reanalysis algorithm using incremental Cholesky factorization and its application to crack growth modeling [J]. *International Journal for Numerical Methods in Engineering*, 2012, **91**: 1358-1364.

[17] Ventura G, Budyn E, Belytschko T. Vector level sets for description of propagating cracks in finite elements [J]. *International Journal for Numerical Methods in Engineering*, 2003, **58**: 1571-1592.